

Published in final edited form as:

Bioconjug Chem. 2009 December ; 20(12): 2342–2347. doi:10.1021/bc900361g.

An Engineered Knottin Peptide Labeled with ^{18}F for PET Imaging of Integrin Expression

Zheng Miao^{1,2,3}, Gang Ren^{1,2,3}, Hongguang Liu^{1,2,3}, Richard H. Kimura^{1,2,4}, Lei Jiang^{1,2,3}, Jennifer R. Cochran^{1,2,4}, Sanjiv Sam Gambhir^{1,2,3,4}, and Zhen Cheng^{1,2,3,*}

¹Molecular Imaging Program at Stanford (MIPS), Stanford University, Stanford California, 94305

²Bio-X Program, Stanford University, Stanford California, 94305

³Department of Radiology, Stanford University, Stanford California, 94305

⁴Department of Bioengineering, Stanford University, Stanford California, 94305

Abstract

Knottins are small constrained polypeptides that share a common disulfide-bonded framework and a triple-stranded β -sheet fold. Previously, directed evolution of the *Ecballium elaterium* trypsin inhibitor (EETI-II) knottin led to the identification of a mutant that bound to tumor-specific $\alpha_v\beta_3$ and $\alpha_v\beta_5$ integrin receptors with low nanomolar affinity. The objective of this study was to prepare and evaluate a radiofluorinated version of this knottin (termed 2.5D) for microPET imaging of integrin positive tumors in living subjects. Knottin peptide 2.5D was prepared by solid phase synthesis and folded *in vitro*, and its free N-terminal amine was reacted with *N*-succinimidyl-4- $^{18/19}\text{F}$ -fluorobenzoate ($^{18/19}\text{F}$ -SFB) to produce the fluorinated peptide $^{18/19}\text{F}$ -FB-2.5D. The binding affinities of unlabeled knottin peptide 2.5D and ^{19}F -FB-2.5D to U87MG glioblastoma cells were measured by competition binding assay using ^{125}I -labeled echistatin. It was found that unlabeled 2.5D and ^{19}F -FB-2.5D competed with ^{125}I -echistatin for binding to cell surface integrins with IC_{50} values of 20.3 ± 7.3 and 13.2 ± 5.4 nM, respectively. Radiosynthesis of ^{18}F -FB-2.5D resulted in a product with high specific activity (ca 100 GBq/ μmol). Next, biodistribution and positron emission tomography (PET) imaging studies were performed to evaluate the *in vivo* behavior of ^{18}F -FB-2.5D. Approximately 3.7 MBq ^{18}F -FB-2.5D was injected into U87MG tumor bearing mice via the tail vein. Biodistribution studies demonstrated that ^{18}F -FB-2.5D had moderate tumor uptake at 0.5 h post injection, and co-injection of a large excess of the unlabeled peptidomimetic c (RGDyK) as a blocking agent significantly reduced tumor uptake (1.90 ± 1.15 vs. 0.57 ± 0.14 %ID/g, 70% inhibition, $P < 0.05$). *In vivo* microPET imaging showed that ^{18}F -FB-2.5D rapidly accumulated in the tumor and quickly cleared from the blood through the kidneys, allowing excellent tumor-to-normal tissue contrast to be obtained. Collectively, ^{18}F -FB-2.5D allows integrin-specific PET imaging of U87MG tumors with good contrast, and further demonstrates that knottins are excellent peptide scaffolds for development of PET probes with potential for clinical translation.

Keywords

Knottin Peptide; Integrin; ^{18}F ; PET; RGD

* Correspondence Should be Sent to: Zhen Cheng, Ph.D, Molecular Imaging Program at Stanford, Department of Radiology and Bio-X Program, 1201 Welch Road, Lucas Expansion, P020A, Stanford University, Stanford, CA 94305, 650-723-7866 (V), 650-736-7925(Fax), zcheng@stanford.edu.

INTRODUCTION

Recent advancement in *in vitro* display technologies (phage, bacterial, yeast, ribosome and mRNA) and rational protein engineering has resulted in many novel peptide-scaffolds that bind to a variety of molecular targets (1-5). Following the discovery of these new affinity ligands, came their adaptation for use in cancer imaging applications (6-7). These small polypeptides can easily be produced by chemical approaches such as solid phase peptide synthesis or generated recombinantly using the tools of molecular biology. Moreover, the small size of these polypeptides generally leads to fast tumor targeting and relatively short *in vivo* half life compared with monoclonal antibodies. Collectively, these properties bode well for nuclear imaging applications with potential for clinical translation.

Cystine knot proteins (also known as knottins) are small constrained polypeptides that share a common disulfide-bonded framework and a triple-stranded β -sheet fold (Figure 1A) (8). Indeed, the scaffold's core structure is very rigid. In general, this class of polypeptides are relatively stable in various physical, chemical and biological environments. Individual family members share little sequence homology except the core cysteine residues. Knottin family members possess one or more surface-exposed loops that tolerate much sequence diversity. These looped regions are responsible for a range of biological activities (9, 10). However, in most cases, their natural functions remain unknown.

Previously, the *Ecballium elaterium* trypsin inhibitor II (EETI-II), a knottin from the squash family of protease inhibitors, was used as a scaffold for directed evolution studies (11). An Arg-Gly-Asp (RGD) integrin binding motif was grafted into a surface-exposed loop, where yeast surface display combined FACS led to the identification of peptides including 2.5D that bound integrin receptors ($\alpha_v\beta_3$, $\alpha_v\beta_5$, and $\alpha_5\beta_1$) with low nanomolar affinities (Figure 1). Near infrared-dye Cy5.5- and ^{64}Cu -DOTA-conjugated knottin peptides were then synthesized and evaluated in mouse xenograft models (12). Biodistribution and micro positron emission tomography (microPET) imaging studies revealed that these engineered knottin peptides performed well *in vivo* and show promise as a new class imaging agent. These peptides demonstrated rapid and high tumor accumulation, fast clearance from blood and normal organs, and low uptake in the kidney and liver (12).

^{18}F is the most commonly used PET radionuclide and has almost ideal physical properties ($t_{1/2}$: 110 min, emits β^+ particles at $E_{\text{max}} = 635$ keV and $E_{\text{ave}} = 250$ keV, 97% abundant) for PET imaging. In this study, to further evaluate the clinical translation ability of engineered knottins, peptide 2.5D was site-specifically labeled with ^{18}F by conjugation with the radiofluorination synthon, *N*-succinimidyl-4- ^{18}F -fluorobenzoate (^{18}F -SFB), through the peptide N-terminus amine (Figure 1). ^{18}F -FB-2.5D was then evaluated in nude mice bearing subcutaneous U87MG xenografts characterized by high levels of integrin expression (13).

EXPERIMENTAL PROCEDURES

General

SFB was obtained from ABX GmbH (Radeberg, Germany). All 9-fluorenylmethyloxycarbonyl (Fmoc) protected amino acids were purchased from Novabiochem/EMD Chemicals Inc (La Jolla, CA) or CS Bio (Menlo Park, CA). ^{125}I -labeled echistatin and c(RGDyK) were purchased from GE Healthcare Life Sciences (Piscataway, NJ), and Peptides International (Louisville, KY), respectively. Phosphate buffered saline (PBS) was from Gibco/Invitrogen (Carlsbad, CA). Echistatin and *N,N'*-diisopropylethylamine (DIPEA) were purchased from Sigma-Aldrich Chemical Co. (St. Louis, MO). All other chemicals were purchased from Thermo Fisher Scientific (Fair Lawn, NJ) unless otherwise specified. The U87MG human glioblastoma cell line was obtained from American Type Culture Collection (Manassas, VA). Nude mice

(nu/nu, female 5–6 weeks old) were purchased from Charles River Laboratory (Wilmington, MA). A CRC-15R PET dose calibrator (Capintec Inc., Ramsey, NJ) was used for all radioactivity measurements. Reverse phase high performance liquid chromatography (RP-HPLC) was performed on a Dionex Summit HPLC system (Dionex Corporation, Sunnyvale, CA) equipped with a 170U 4-Channel UV-Vis absorbance detector and radioactivity detector (Carroll & Ramsey Associates, model 105S, Berkeley, CA). UV detection wavelengths were 218 nm, 254 nm and 280 nm for all the experiments. Both semi-preparative (Vydac, Hesperia, CA. 218TP510-C18, 10 mm × 250 mm) and analytical (Dionex, Sunnyvale, CA. Acclaim120 C18, 4.6 mm × 250 mm) RP-HPLC columns were used. The mobile phase was solvent A, 0.1% trifluoroacetic acid (TFA)/H₂O, and solvent B, 0.1% TFA/acetonitrile. Matrix-assisted laser desorption/ionization time of flight mass spectrometry (MALDI-TOF-MS) were performed on a Perseptive Voyager-DE RP Biospectrometry instrument (Framingham, MA) by the Stanford Protein and Nucleic Acid Biotechnology Facility (Stanford, CA).

Chemistry and Radiochemistry

Peptide 2.5D was synthesized on a CS Bio CS336 instrument (Menlo Park, CA) using Fmoc-based solid phase peptide synthesis method. Briefly, Rink amide resin was swollen in *N,N*-dimethylformamide (DMF) for 30 min. Fmoc groups were removed with 20% piperidine in DMF. Aliquots of amino acids (1 mmol) were activated in a solution containing 1 mmol of hydroxybenzotriazole (HOBt) and 0.5 M diisopropylcarbodiimide (DIC) in DMF. Following synthesis, side-chain deprotection and resin cleavage was achieved by addition of a 94:2.5:2.5:1 (v/v) mixture of trifluoroacetic acid (TFA) : trimethylsilane : ethanedithiol : water for 2 h at room temperature. The crude product was precipitated with cold anhydrous diethyl ether, and purified by a preparative or semi-preparative RP-HPLC using a Varian Prostar instrument and Vydac C₁₈ columns. Peptide purity was analyzed by analytical scale RP-HPLC using a Vydac C₁₈ column.

Folding reactions were performed by incubating the linear peptide with 2.5 mM reduced glutathione and 20% dimethyl sulfoxide (DMSO) in 0.1 M ammonium bicarbonate, pH 9, with gentle rocking. The final oxidized product was purified by RP-HPLC as described above; the folded knottin peptide exhibited a distinct chromatographic profile that allowed it to be separated from unfolded and misfolded isomers (11). Following purification, folded peptide 2.5D was lyophilized and stored at room temperature until used. Purified peptide was dissolved in water, and concentration was determined by amino acid analysis (Molecular Structure Facility, Davis, CA). Peptide purity and molecular mass were determined by analytical scale RP-HPLC and MALDI-TOF-MS or ESI-MS.

Non-radioactive ¹⁹F-FB-2.5D, a reference standard, was prepared by reaction of knottin peptide 2.5D with SFB. Briefly, 0.15 μmol of knottin peptide 2.5D (0.5 mg in 400 μL of DMSO) was mixed with 1.5 μmol of SFB (0.36 mg in 100 μL of DMSO) and 30 μL of DIPEA and reacted for 1 h at 60 °C. The resulting conjugate ¹⁹F-FB-2.5D was then purified by RP-HPLC on a semi-preparative C₁₈ column using a gradient system of 0.1% trifluoroacetic acid in acetonitrile (solvent B) and 0.1% trifluoroacetic acid in water (solvent A). The flow rate was 3 mL/min, with the mobile phase starting from 90% solvent A and 10% solvent B (0–3 min) to 35% solvent A and 65% solvent B at 33 min. Fractions containing the product were collected and lyophilized. The identity of ¹⁹F-FB-2.5D was confirmed by MALDI-TOF-MS.

¹⁸F-SFB was prepared based on a previously reported procedure (14). The specific activity of ¹⁸F-SFB was 200–250 GBq/μmol at the end of synthesis (EOS), as estimated by radio-HPLC. Radiolabeling agent ¹⁸F-SFB in 100 μL of DMSO was added to knottin peptide 2.5D (100 μg, in 100 μL of DMSO) and 10 μL of DIPEA and reacted for 1 h at 60 °C. After adding 50 μL of TFA to quench the reaction, the mixture was purified with semi-preparative HPLC, using the same elution gradient as for the cold ¹⁹F-FB-2.5D purification. The eluted fractions

containing the ^{18}F -FB-2.5D were then collected, combined, and dried using a rotary evaporator. The radiolabeled peptide was reconstituted in PBS (0.01 M, pH 7.4) and passed through a 0.22- μm Millipore filter into a sterile vial for cell culture and animal experiments.

Octanol/Water Partition Coefficient

To determine the hydrophilicity of ^{18}F -FB-2.5D, approximately 370 kBq of the probe in 500 μl of PBS (0.01 M, pH 7.4) was added to 500 μl of octanol in a microcentrifuge tube. The resulting biphasic system was mixed vigorously for 0.5 h and left at room temperature for another 0.5 h. The two phases were then separated by centrifugation at 3000 g for 5 min (model 5415R Eppendorf microcentrifuge; Brinkman, Westbury, NY). An aliquot of 100 μl was removed from each layer and analyzed in a γ -counter (model 1470; PerkinElmer). The partition coefficient ($\log P$) was then calculated as a ratio of counts in the octanol fraction to the counts in the water fraction. The experiment was repeated 3 times.

Cell Culture

U87MG cells were cultured in DMEM containing high glucose (Gibco, Carlsbad, CA), which was supplemented with 10% fetal bovine serum (FBS) and 1% penicillin-streptomycin. The cells were expanded in tissue culture dishes and kept in a humidified atmosphere of 5% CO_2 at 37 $^\circ\text{C}$. The media was changed every other day. A confluent monolayer was detached with 0.5% Trypsin-EDTA, 0.01M PBS (pH 7.4) and dissociated into a single-cell suspension for further cell culture and assays.

U87MG Cell Binding Assay

This assay was performed as previously described (11,12). Briefly, 2×10^5 U87MG cells were incubated with 0.06 nM ^{125}I -labeled echistatin and varying concentrations of compounds (echistatin, knottin 2.5D, ^{19}F -FB-2.5D) in integrin binding buffer [IBB, 25 mM Tris pH 7.4, 150 mM NaCl, 2mM CaCl_2 , 1 mM MgCl_2 , 1 mM MnCl_2 , and 0.1% bovine serum albumin (BSA)] at room temperature for 3 h. The cell-bound radioactivity remaining after washing was determined by gamma-counting. IC_{50} values, the concentration of competitor required to inhibit 50% of the radioligand binding, were determined by non-linear regression analysis using Kaleidagraph (Synergy Software, Reading, PA), and are presented as the average of three experiments performed.

Animal Biodistribution Studies

All animal studies were carried out in compliance with Federal and local institutional rules for the conduct of animal experimentation. Approximately 10×10^6 cultured U87MG cells were suspended in PBS and subcutaneously implanted in the left shoulders of nude mice. Tumors were allowed to grow to a size of 0.5 cm (2-3 weeks) before imaging experiments. For biodistribution studies, mice bearing U87MG xenografts ($n = 3$ for each group) were injected with approximately 740 KBq (20 μCi) of ^{18}F -FB-2.5D with or without 330 μg of unlabeled c (RGDyK) via the tail vein and sacrificed at 0.5 h post injection (p.i.). Tumor and normal tissues of interest were removed and weighed, and their radioactivity was measured in a gamma-counter. The radioactivity uptake in the tumor and normal tissues was expressed as a percentage of the injected radioactive dose per gram of tissue (% ID/g).

MicroPET Imaging

Mice bearing U87MG xenografts were injected with approximately 4.44 MBq (120 μCi) of ^{18}F -FB-2.5D with or without 330 μg of c(RGDyK) via the tail vein and PET imaging was performed using a microPET R4 rodent model scanner (Siemens Medical Solutions USA, Inc., Knoxville, TN). At 0.5 and 1 h p.i., mice were anesthetized with isoflurane (5% for induction and 2% for maintenance in 100% O_2). With the help of a laser beam attached to the scanner,

mice were placed in the prone position and near the center of the field of view of the scanner and 3-min static scans were obtained. For dynamic scanning, approximately 3.7MBq (100 μ Ci) of ^{18}F -FB-2.5D was injected into U87MG tumor-bearing mice via the tail vein and a 35 min duration dynamic scan (10×1 min, 10×2 min, 1×5 min; total of 21 frames) was started approximately 2.5 min after injection of the probe. Images were reconstructed by a two-dimensional ordered-subsets expectation maximization (OSEM) algorithm. No background correction was performed. Region of interests (ROIs; 5 pixels for coronal and transaxial slices) were drawn over the tumor on decay-corrected whole-body coronal images. The maximum counts per pixel per minute were obtained from the ROIs and were converted to counts per milliliter per minute using a calibration constant. ROIs were then converted to counts per gram per minute based on the assumption of a tissue density of 1 gram/ml, and image ROI-derived %ID/g values were determined by dividing counts per gram per minute by injected dose. No attenuation correction was performed.

Statistical Method

Statistical analysis was performed using the Student's *t*-test for unpaired data. A 95% confidence level was chosen to determine the significance between groups, with $P < 0.05$ being designated as significantly different.

RESULTS

Chemistry and Radiochemistry

Knottin peptide 2.5D was synthesized in two steps. First, the linear peptide was prepared by conventional solid phase peptide synthesis and purified by RP-HPLC. Next, the peptide was oxidatively folded using a mixture of glutathione and DMSO and the final oxidized product was purified by semi-preparative reversed-phase HPLC (11). The folded peptide was obtained in ~10% yield with >95% purity. Reaction of SFB with the N-terminal amine of knottin peptide 2.5D generated ^{19}F -FB-2.5D, a non-radioactive species, as a reference compound for cell binding affinity studies. For all knottin peptides prepared above, the measured molecular weights were consistent with the expected masses. 2.5D Linear peptide: $m/z = 3249.6$ Da for $[\text{M}+\text{H}]^+$ (calculated $[\text{M}+\text{H}]^+ = 3249.6$ Da); 2.5D folded peptide: $m/z = 3243.8$ Da for $[\text{M}+\text{H}]^+$ (calculated $[\text{M}+\text{H}]^+ = 3243.6$ Da); ^{19}F -FB-2.5D: $m/z = 3365.7$ Da for $[\text{M}+\text{H}]^+$ (calculated $[\text{M}+\text{H}]^+ = 3365.7$ Da).

Similarly, ^{18}F -FB-2.5D was synthesized by coupling knottin peptide 2.5D with radiosynthon ^{18}F -SFB. Radiolabeled ^{18}F -FB-2.5D, which had a retention time of 20.2 minutes, was easy to differentiate by RP-HPLC compared to unlabeled knottin peptide 2.5D, which had a retention time of 16.9 minutes. Radiosynthesis and purification of ^{18}F -FB-2.5D was completed in approximately 3 hours, which is important for experimental use due to the short half-life of ^{18}F . The maximum overall radiochemical yield with decay correction was 28.3% at EOS. The radiochemical purity of the labeled peptide was over 95% as verified by analytic HPLC analysis (Figure 2). An octanol/water distribution study performed on ^{18}F -FB-2.5D showed good hydrophilicity with a partition coefficient number ($\log P$) of -1.68.

U87MG Cell Binding Assay

The relative binding affinities of 2.5D and ^{19}F -FB-2.5D to cell surface integrin receptors were determined through a competition binding assay with ^{125}I -echistatin. Echistatin, a snake venom protein that binds to $\alpha_v\beta_3$ integrin with $K_D \sim 0.3$ nM, was also used as the positive control (15). Both knottin peptides inhibited the binding of ^{125}I -echistatin to integrin-expressing U87MG cells in a concentration-dependent manner (Figure 3). The mean \pm standard deviation IC_{50} values of 2.5D, ^{19}F -FB-2.5D and echistatin were 20.3 ± 7.3 nM, 13.2 ± 5.4 nM, and 3.7

± 1.1 nM, respectively. These studies indicate that conjugation of fluorobenzoic acid moiety to the N-terminus of knottin peptide 2.5D doesn't reduce its integrin binding affinity.

Biodistribution Studies

The *in vivo* biodistribution of ^{18}F -FB-2.5D was next performed in mice bearing U87MG human glioblastoma xenografts 0.5 h p.i. (Figure 4). Radiolabeled ^{18}F -FB-2.5D displayed moderate accumulation in U87MG tumors (1.90 ± 1.15 %ID/g at 0.5 h p.i.). Kidney and liver uptake were 4.24 ± 0.19 and 1.38 ± 0.55 %ID/g, respectively. Lower levels of radioactivity were observed in blood (1.32 ± 0.07 %ID/g) and the most other organs. To measure integrin specificity, ^{18}F -FB-2.5D was co-injected with an excess (330 μg) of the unlabeled c(RGDyK) to block integrin binding sites. Co-injection of c(RGDyK) specifically reduced the tumor uptake of ^{18}F -FB-2.5D to 0.57 ± 0.14 %ID/g (70% inhibition, $P < 0.05$), without changing the distribution of the probe in most normal tissues studied.

MicroPET Imaging

The *in vivo* tumor targeting profile of ^{18}F -FB-2.5D was further investigated in U87MG tumor-bearing nude mice by dynamic microPET scanning over a 35 minute time period. As shown in Figure 5A, ^{18}F -FB-2.5D rapidly accumulated in the tumor and reached a maximum of 3.5 %ID/g at 5 min p.i. and gradually decreased to 1.73 %ID/g over the duration of the 35 min scan. The scan revealed relatively low radioactivity in the muscle. Lung uptake was high at early time points and rapidly washed out to 1.09 %ID/g at 35 min p.i. Rapid blood clearance of the probe was determined by ROI analysis of the heart. At 35 min p.i., radioactivity in the blood was approximately 9.2% of the amount observed at 3 min p.i. (Figure 5B). High kidney uptake was observed at early time points (for example, 51.8 %ID/g at 4 min p.i.), but this activity rapidly cleared out and dropped to 6.2 %ID/g at 35 min p.i.. ^{18}F -FB-2.5D displayed relatively low liver uptake, in agreement with previous data on knottin peptides (12). Collectively, these data indicate that ^{18}F -FB-2.5D was mainly cleared through the renal system.

Representative decay-corrected coronal (top) and transaxial (bottom) microPET images of nude mice bearing U87MG tumors on their left shoulder at 0.5 and 1 h after tail vein injection of 4.44 MBq (120 μCi) of ^{18}F -FB-2.5D are shown in Figure 6. The U87MG tumor was clearly delineated with good tumor to contralateral background contrast at 0.5 and 1 h p.i. (left and right images in Figure 6). Moreover, co-injection of an excess of c(RGDyK) peptide reduced the tumor uptake of ^{18}F -FB-2.5D, resulting in lower tumor to background contrast at 0.5 h (middle images in Figure 6). Finally, relatively high activities were observed in the bladder and gallbladder. Quantitative analyses were performed on microPET images (Figure 7). Tumor uptake values were determined to be 2.60 ± 0.72 %ID/g at 0.5 h p.i., and decreased to 1.46 ± 0.35 %ID/g at 1 h p.i. Co-injection of c(RGDyK) significantly blocked uptake of the radiotracer in the tumor to 0.61 ± 0.14 %ID/g ($P < 0.05$) at 0.5 h p.i., which agreed well with biodistribution results.

DISCUSSION

Novel non-immunogenic scaffold-based polypeptides have drawn a lot of attention for the development of molecular imaging probes because of easy synthesis, site-specific labeling, stable structure and high versatility targeting various cancer biomarkers. In our recent work, an anti-human epidermal growth factor receptor type 2 (HER2) Affibody molecule, engineered from one IgG binding domain of protein A and $\sim 1/20$ size of an antibody, was site-specifically labeled with ^{18}F . The resulting probe demonstrated great potential for PET imaging of the expression of HER2 in the clinic (16). HER2 Affibody molecules have also been labeled with many other radioisotopes and organic dyes for preclinical and clinical imaging (17-19). These

progressions in scaffold protein based molecular probe development have motivated us to explore other scaffold protein as molecular platforms targeting different biomarkers.

The cystine knot miniprotein family represents a unique peptide scaffold of ~ 3 kDa with three interwoven disulfide bridges. Engineered knottin peptides, such as the integrin-binding peptide 2.5D, have been identified and their potential for *in vivo* integrin molecular imaging has recently been evaluated as a ^{64}Cu -labeled PET tracer (12). Preliminary evaluation of ^{64}Cu -labeled knottin peptides showed excellent tumor imaging properties in living mice. To facilitate the translation of knottin peptides as clinical imaging agents, we next tested an ^{18}F -labeled version of knottin peptide 2.5D in tumor-bearing mouse models in this research. With these studies, we wanted to determine whether there are any advantages and disadvantages of using knottin scaffolds as imaging agents as well as to further enrich our understanding of the *in vivo* behavior of knottin peptides when they are coupled with different radionuclides.

In this research, ^{18}F -SFB was used as a prosthetic group for site-specifically labeling knottin 2.5D (Figure 1). Methods to couple ^{18}F -SFB have been well-established in our program (14). The non-radioactive version, ^{19}F -FB-2.5D, competes with ^{125}I -echistatin for binding cell surface integrins with an IC_{50} of 13.2 ± 5.4 nM, which is similar to that of the unmodified knottin peptide 2.5D (20.3 ± 7.3 nM). These data suggest that the N terminal amine of the knottin peptide tolerates modification, and further *in vivo* evaluation of its radioactive counterpart confirmed this finding. Radiofluorination of 2.5D was efficiently achieved through site-specific conjugation of the radiosynthon, ^{18}F -SFB, with the N terminus amino group under mild conditions (60°C , 1 h). ^{18}F -FB-2.5D was prepared in a reasonable yield (final yield, 28.3%) and high specific activity (~ 100 GBq/ μmol) at EOS, which bode well for clinical applications.

Considering the short physical half life of ^{18}F as well as short biological blood half life of the knottin peptide, our biodistribution and imaging data of ^{18}F -FB-2.5D were acquired in a relatively short time frame (up to 1 h p.i.). Consistent with our expectation, we observed good tumor uptake resulting in good image quality. These data are attributable to peptide's tumor targeting ability and rapid clearance from normal tissues (Figure 4). As early as 0.5 h p.i., probe uptake in the tumor was 1.90 ± 1.15 %ID/g. Liver uptake remained low at around 1.4 ± 0.5 %ID/g at 0.5 h, which was similar compared with its ^{64}Cu labeled knottin counterpart (2.3 ± 0.8 %ID/g) (12). Overall, microPET imaging data correlated well with the data derived from biodistribution studies. The U87MG tumor is clearly delineated from normal tissue at both 0.5 and 1 h p.i.. Quantification of microPET images showed that 56% of the activity remained in the tumor 1 h p.i., compared to the 0.5 h time point. Dynamic PET scans showed that the majority of ^{18}F -FB-2.5D was quickly cleared through renal system, and the blood radioactivity concentration dropped dramatically in the first 35 min p.i. These pharmacokinetic properties suggest translational potential.

Integrin $\alpha_v\beta_3$ expression *in vivo* has extensively been imaged by small, backbone cyclized peptidomimetics [c(RGDyK), c(RGDfK), etc.] (20-24). ^{18}F -FB labeled c(RGDyK) [abbreviated as FB-RGD] was reported to moderately target U87MG tumors *in vivo* (ca 3 and 2.5 %ID/g uptake at 0.5 and 1 h, respectively) (21). ^{18}F -FB-2.5D demonstrated lower liver uptake (1.5 %ID/g at 0.5 h p.i.) compared to ^{18}F -FB-RGD (ca 2.5 and 1 %ID/g at 0.5). But ^{18}F -FB-2.5D has lower tumor uptake (ca 2 % ID/g at 0.5 h p.i.) and the kidney uptake is slightly higher than ^{18}F -FB-RGD (4.5 vs. 3.5 %ID/g at 0.5 h p.i.). The findings presented here are different from our previous experience. In our recent report, ^{64}Cu labeled DOTA-2.5D did show significant advantages over ^{64}Cu -DOTA-c(RGDyK) (12). This difference indicates that various labeling methods impact *in vivo* performance of knottins. Moreover, it suggests that further optimization of ^{18}F -FB-2.5D may lead to a radiofluorinated knottin probe with improved properties. It was reported that PEGylation enhanced the tumor uptake and prolonged

the retention of ^{18}F labeled c(RGDyK) (ca 5 %ID/g at 0.5 h and 2.5 %ID/g at 2 h p.i.), while the liver uptake remained the same (ca 2.6 %ID/g at 0.5 h) (24). Similar strategies could be adapted to improve the tumor uptake and retention of ^{18}F -labeled knottins and increase the tumor-to-liver ratios.

As an important target for cancer therapy, $\alpha_v\beta_3$ integrin is highly overexpressed on tumor cells and the tumor neovasculature of many cancer including melanoma and glioblastoma (13,25, 26). An optimized ^{18}F labeled 2.5D probe could be used for diagnosis of $\alpha_v\beta_3$ -positive tumors, both at primary and metastatic sites. ^{18}F -labeled 2.5D could also be used for stratification of patients, detection of cancer recurrence, and for monitoring therapeutic efficacy of integrin-targeted drugs. In Conclusion, radiolabeled knottin peptide ^{18}F -FB-2.5D allows integrin-specific PET imaging of U87MG tumors with good contrast, and is mainly cleared from the body through the renal system. Knottins are excellent peptide scaffolds for the development of PET probes for clinical translation.

Acknowledgments

This work was supported, in part, by Department of Radiology, Stanford University (ZC), National Cancer Institute (NCI) In Vivo Cellular Molecular Imaging Center (ICMIC) grant P50 CA114747 (SSG), NCI Small Animal Imaging Resource Program (SAIRP) grant R24 CA93862, NCI 5R01 CA119053 (ZC), NCI 5K01 CA104706 (JRC), and the Edward Mallinckrodt Jr. Foundation (JRC). The Stanford University cyclotron team, particularly Fred Chin is acknowledged for radionuclide production.

References

1. Rothe A, Hosse RJ, Power BE. In vitro display technologies reveal novel biopharmaceuticals. *FASEB J* 2006;20:1599–1610. [PubMed: 16873883]
2. Hosse RJ, Rothe A, Power BE. A new generation of protein display scaffolds for molecular recognition. *Protein Sci* 2006;15:14–27. [PubMed: 16373474]
3. Uchiyama F, Tanaka Y, Minari Y, Tokui N. Designing scaffolds of peptides for phage display libraries. *J Biosci Bioeng* 2005;99:448–456. [PubMed: 16233816]
4. Nygren PA, Skerra A. Binding proteins from alternative scaffolds. *J Immunol Methods* 2004;290:3–28. [PubMed: 15261569]
5. Binz HK, Amstutz P, Pluckthun A. Engineering novel binding proteins from nonimmunoglobulin domains. *Nat Biotechnol* 2005;23:1257–1268. [PubMed: 16211069]
6. Orlova A, Feldwisch J, Abrahmsén L, Tolmachev V. Update: affibody molecules for molecular imaging and therapy for cancer. *Cancer Biother Radiopharm* 2007;22:573–584. [PubMed: 17979560]
7. Ladner RC. Polypeptides from phage display: A superior source of in vivo imaging agents. *Q J Nucl Med* 1999;43:119–124. [PubMed: 10429506]
8. Pallaghy PK, Nielsen KJ, Craik DJ, Norton RS. A common structural motif incorporating a cystine knot and a triple-stranded beta-sheet in toxic and inhibitory polypeptides. *Protein Sci* 1994;3:1833–1839. [PubMed: 7849598]
9. Chiche L, Heitz A, Gelly JC, Gracy J, Chau PT, Ha PT, Hernandez JF, Le-Nguyen D. Squash inhibitors: from structural motifs to macrocyclic knottins. *Curr Protein Pept Sci* 2004;5:341–349. [PubMed: 15551519]
10. Craik DJ, Daly NL, Waine C. The cystine knot motif in toxins and implications for drug design. *Toxicon* 2001;39:43–60. [PubMed: 10936622]
11. Kimura RH, Levin AM, Cochran FV, Cochran JR. Engineered cystine knot peptides that bind $\alpha_v\beta_3$, $\alpha_v\beta_5$, and $\alpha_5\beta_1$ integrins with low-nanomolar affinity. *Proteins* 2009;77:359–369. [PubMed: 19452550]
12. Kimura RH, Cheng Z, Gambhir SS, Cochran JR. Engineered knottin peptides: a new class of agents for imaging integrin expression in living subjects. *Cancer Res* 2009;69:2435–2442. [PubMed: 19276378]

13. Zako T, Nagata H, Terada N, Utsumi A, Sakono M, Yohda M, Ueda H, Soga K, Maeda M. Cyclic RGD peptide-labeled upconversion nanophosphors for tumor cell-targeted imaging. *Biochem Biophys Res Commun* 2009;381:54–58. [PubMed: 19351594]
14. Cheng Z, Zhang L, Graves E, Xiong Z, Dandekar M, Chen X, Gambhir SS. Small-animal PET of melanocortin 1 receptor expression using a ^{18}F -labeled alpha-melanocyte-stimulating hormone analog. *J Nucl Med* 2007;48:987–994. [PubMed: 17504880]
15. Kumar CC, Nie H, Rogers CP, Malkowski M, Maxwell E, Catino JJ, Armstrong L. Biochemical characterization of the binding of echistatin to integrin $\alpha\text{v}\beta\text{3}$ receptor. *J Pharmacol Exp Ther* 1997;283:843–853. [PubMed: 9353406]
16. Cheng Z, Padilla De Jesus O, Namavari M, De A, Levi J, Webster JM, Zhang R, Lee B, Syud FA, Gambhir SS. Small-animal PET imaging of human epidermal growth factor receptor type 2 expression with site-specific ^{18}F -labeled protein scaffold molecules. *J Nucl Med* 2008;49:804–813. [PubMed: 18413392]
17. Lee SB, Hassan M, Fisher R, Chertov O, Chernomordik V, Kramer-Marek G, Gandjbakhche A, Capala J. Affibody molecules for in vivo characterization of HER2-positive tumors by near-infrared imaging. *Clin Cancer Res* 2008;14:3840–3849. [PubMed: 18559604]
18. Baum R, Orlova A, Tolmachev V, Feldwisch J. Receptor PET/CT and SPECT using an Affibody molecule for targeting and molecular imaging of HER2-positive cancer in animal xenografts and human breast cancer patients [abstract]. *J Nucl Med* 2006;47(suppl):108.
19. Engfeldt T, Orlova A, Tran T, Bruskin A, Widström C, Karlström AE, Tolmachev V. Imaging of HER2-expressing tumours using a synthetic Affibody molecule containing the $^{99\text{m}}\text{Tc}$ -chelating mercaptoacetyl-glycyl-glycyl-glycyl (MAG3) sequence. *Eur J Nucl Med Mol Imaging* 2007;34:722–733. [PubMed: 17146656]
20. Cheng Z, Wu Y, Xiong Z, Gambhir SS, Chen X. Near-infrared fluorescent RGD peptides for optical imaging of integrin $\alpha\text{v}\beta\text{3}$ expression in living mice. *Bioconjug Chem* 2005;16:1433–1441. [PubMed: 16287239]
21. Chen X, Park R, Shahinian AH, Tohmea M, Khankaldyyanb V, Bozorgzadeha MH, Badinga JR, Moatsb R, Laugb WE, Contia RS. ^{18}F -labeled RGD peptide: initial evaluation for imaging brain tumor angiogenesis. *Nucl Med Biol* 2004;31:179–189. [PubMed: 15013483]
22. Zhang X, Xiong Z, Wu Y, Cai W, Tseng JR, Gambhir SS, Chen X. Quantitative PET imaging of tumor integrin $\alpha\text{v}\beta\text{3}$ expression with [^{18}F]FRGD₂. *J Nucl Med* 2006;47:113–121. [PubMed: 16391195]
23. Cai W, Gambhir SS, Chen X. Multimodality tumor imaging targeting integrin $\alpha\text{v}\beta\text{3}$. *BioTechniques* 2005;39:S6–S17.
24. Chen X, Park R, Khankaldyyan V, Tohme M, Bading JR, Laug WE, Conti PS. MicroPET Imaging of Brain Tumor Angiogenesis with ^{18}F -Labeled PEGylated RGD Peptide. *Eur J Nucl Med Mol Imaging* 2004;31:1081–1089. [PubMed: 15118844]
25. Putnam AJ, Schulz VV, Freiter EM, Bill HM, Miranti CK. Src, PKC α , and PKC δ are required for $\alpha\text{v}\beta\text{3}$ integrin-mediated metastatic melanoma invasion. *Cell Commun Signal* 2009;7:10. [PubMed: 19400942]
26. Skuli N, Monferran S, Delmas C, Favre G, Bonnet J, Toulas C, Cohen-Jonathan Moyal E. $\alpha\text{v}\beta\text{3}/\alpha\text{v}\beta\text{5}$ integrins-FAK-RhoB: a novel pathway for hypoxia regulation in glioblastoma. *Cancer Res* 2009;69:3308–3316. [PubMed: 19351861]

Abbreviations

PET	positron emission tomography
HPLC	high-performance liquid chromatography
pi	postinjection

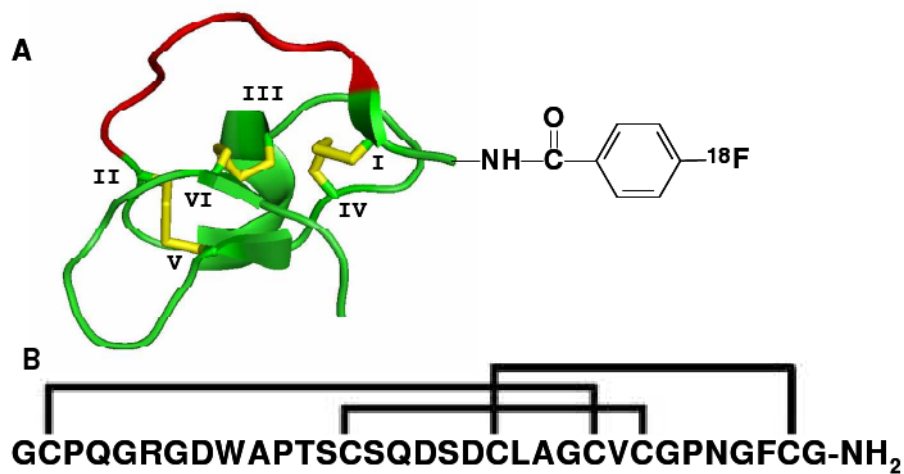


Figure 1. Schematic and sequence of engineered knottin peptides. (A) Cartoon representation of knottin peptide scaffold. The imaging label ¹⁸F-FB was site-specifically conjugated to the N terminal amino group. (B) Amino acid sequence integrin-binding knottin peptide 2.5D with disulfide bonds between Cys1-Cys4, Cys2-Cys5, and Cys3-Cys6.

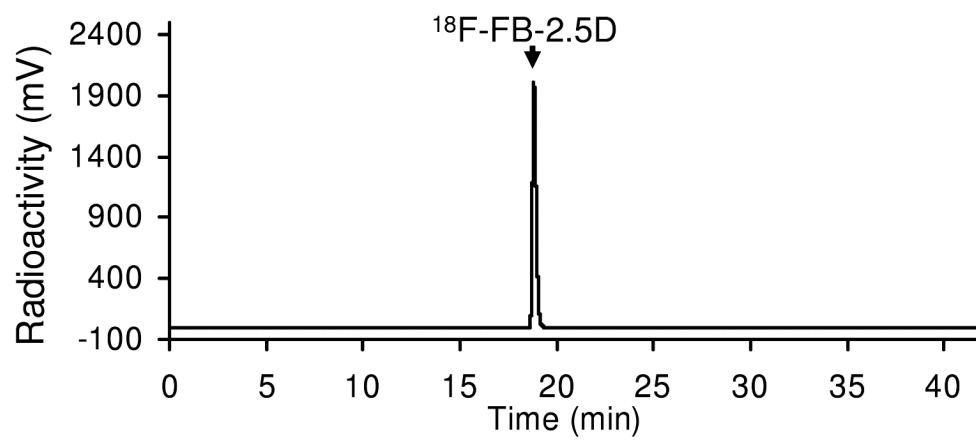


Figure 2.
HPLC radiochromatogram of purified $^{18}\text{F-FB-2.5D}$.

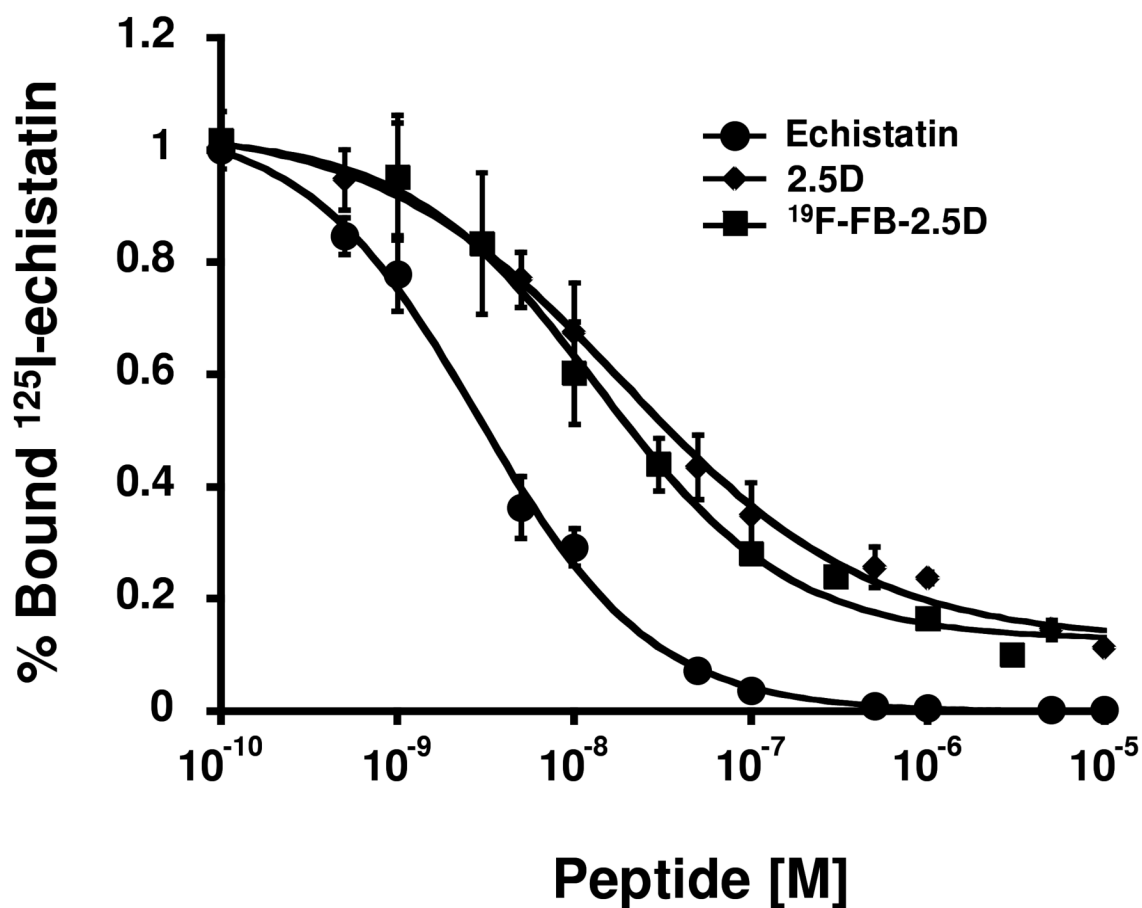


Figure 3. Inhibition of ^{125}I -echistatin binding to integrin receptors on U87MG cells by 2.5D, ^{19}F -FB-2.5D, and echistatin [$\text{IC}_{50} = 20.3 \pm 7.3$ (◆), 13.2 ± 5.4 (■) and 3.7 ± 1.1 (●) nM, respectively). Results are expressed as the percentage of ^{125}I -echistatin binding, and are the mean of triplicate measurements \pm SD.

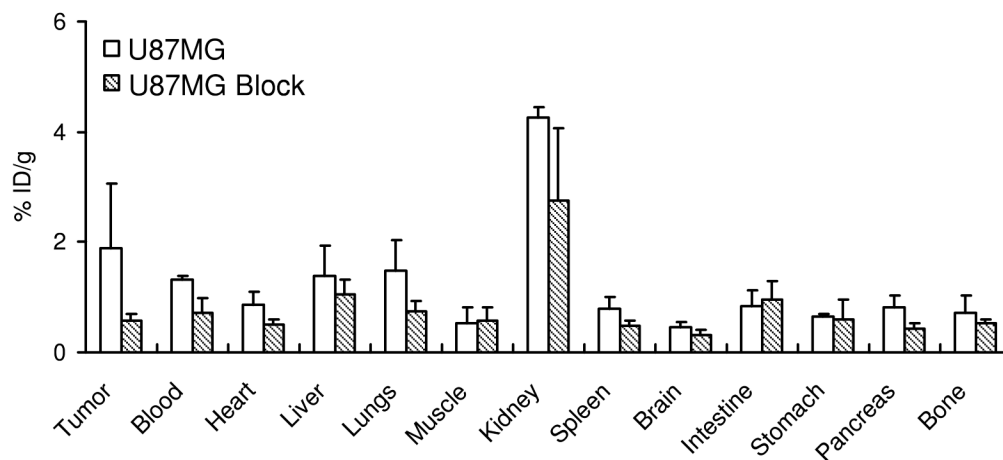


Figure 4. Biodistribution data for ^{18}F -FB-2.5D in nude mice bearing subcutaneous U87MG human tumor xenografts. Data are expressed as the percentage administered activity (injected dose) per gram of tissue (%ID/g) after intravenous injection of 370 kBq (10 μCi) ^{18}F -FB-2.5D at 0.5 h p.i. with or without co-injection of 330 μg of c(RGDyK) ($n = 3$ for each group). Significant inhibition of U87MG tumor uptake ($P < 0.05$) was observed upon co-injection of this blocking agent.

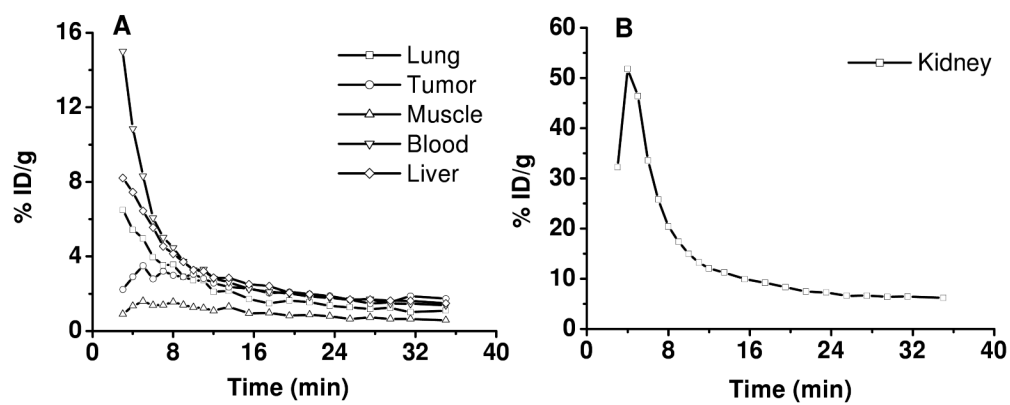


Figure 5. Time activity curves of major organs derived from a microPET dynamic scan of a mouse bearing U87MG tumors, after intravenous injection of $\sim 3.7\text{MBq}$ ($\sim 100\ \mu\text{Ci}$) ^{18}F -FB-2.5D.

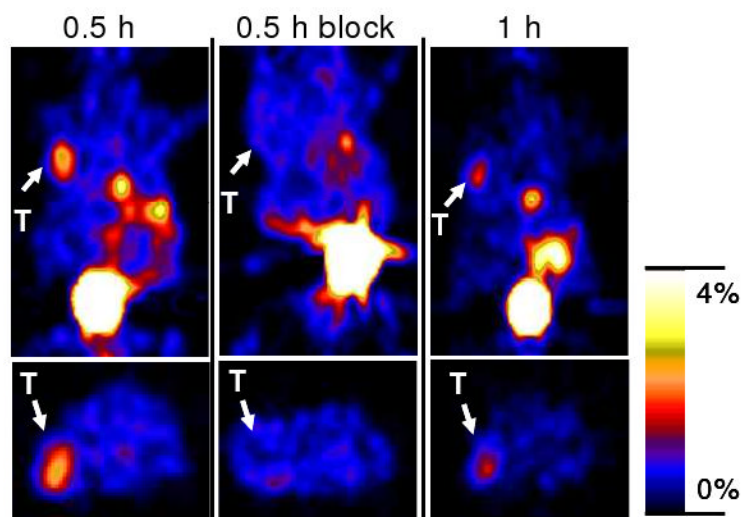


Figure 6. Decay corrected coronal (top) and transaxial (bottom) microPET images of nude mice bearing U87MG tumors (unit: %ID/g). Images were acquired 0.5 and 1 h after tail vein injection of 4.44 MBq (120 μ Ci) of 18 F-FB-2.5D with or without co-injection of 330 μ g of c(RGDyK) ($n = 3$ for each group). Arrows indicate the location of tumors (T). Gallbladder and bladder can also be clearly seen.

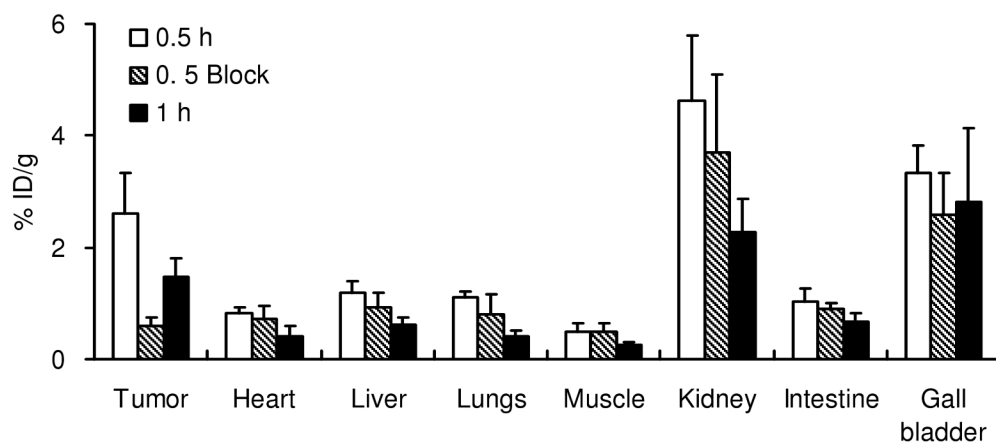


Figure 7. PET imaging quantification of intravenously injected ^{18}F -FB-2.5D measured by using ROI analysis of static small-animal PET data sets in nude mice bearing U87MG tumors ($n = 3$).